Designing an Autonomous Mobile Robot Featuring Self-Localization through 3D LiDAR Technology

Sayat Ibrayev
Joldasbekov Institute of Mechanics and Engineering, Almaty, Kazakhstan
sayattibiray@gmail.com

Batyrkhan Omarov
International Information Technology University, Almaty, Kazakhstan | Al-Farabi Kazakh National University, Almaty, Kazakhstan | Kh. Dosmukhamedov Atyrau State University, Atyrau, Kazakhstan
b.omarov@iitu.edu.kz (corresponding author)

Received: 28 June 2025 | Revised: 2 August 2025 | Accepted: 14 August 2025

 DOI: https://doi.org/10.48084/etasr.13014

ABSTRACT

This paper undertakes a deep investigation into the fabrication of a navigation system in which complex environments pose challenges for accuracy, reliability, and adaptability. With the help of the latest sensor fusion techniques, reliable adaptive algorithms, and machine learning models, our proposed system outperforms existing localization techniques, such as those presented in Autoware's 3D Simultaneous Localization and Mapping (SLAM) and Normal Distribution Transform (NDT) matching. The system empirically demonstrates effectiveness compared with existing methods through the collection of data during manual trolley relocation experiments and Robotic Operating System (ROS) simulations. This process demonstrates an enhancement of both indoor and outdoor navigation performance. Through the simultaneous utilization of multiple sensors, augmented with real-time dynamic self-adjustments and pattern recognition capabilities, the system exhibits outstanding adaptability to individual environmental conditions, resulting in consistent performance across different operating scenarios. This satisfies the requirement for accurate environmental information in autonomous navigation and addresses the challenges of localization accuracy and adaptability, making a comprehensive impact on the development of autonomous vehicles, robotic systems in manufacturing environments, and other domains. Additionally, the outcomes of this investigation broaden the perspective on the operation and application of autonomous technologies, enhancing the safety, efficiency, and reliability of operations in dynamically changing technological environments.

Keywords-mobile robots; autonomous navigation; localization systems; sensor fusion techniques; 3D-SLAM technology; environmental adaptability

I. INTRODUCTION

The rapid advancement of Autonomous Mobile Robots (AMRs) marks a transformative stage in robotics and automation, pushing these systems toward enhanced efficiency, adaptability, and intelligence. Central to this progress is the development of advanced self-localization technologies, enabling robots to operate reliably in complex, dynamic, and unpredictable environments. Among various sensing modalities, 3D Light Detection and Ranging (3D LiDAR) stands out for its exceptional precision, extended range, and versatility compared to alternative solutions [1]. This study addresses two core phases: designing a 3D LiDAR-based self-localization system for an AMR and implementing it, focusing on theoretical foundations, technical design aspects, and associated challenges.

Autonomy in AMRs is achieved through the integration of hardware and software subsystems, with self-localization forming the foundation for essential functions such as path planning, obstacle avoidance, and task execution. Reliable localization, however, is challenging due to environmental variability and the presence of unforeseen obstacles. Traditional methods such as the Global Positioning System (GPS) and ultrasonic sensors, while valuable, suffer from accuracy limitations in indoor or obstructed environments and are vulnerable to environmental interference [2]. By contrast, 3D LiDAR generates high-resolution spatial data for building detailed three-dimensional maps, enabling accurate environmental perception and precise localization [3]. Its adoption has marked a significant leap forward in improving autonomy and operational efficiency [4].

The design of a 3D LiDAR-based AMR involves careful hardware selection, robust data processing algorithms, and efficient system integration. The choice of the LiDAR sensor affects the field of view, range, and resolution, whereas processing its output demands algorithms capable of noise mitigation, managing incomplete datasets, and meeting real-time computational requirements [5].

Simultaneous Localization and Mapping (SLAM) is a widely used approach for 3D LiDAR-based localization, enabling the robot to construct or update a map of an unknown environment while tracking its position [6]. SLAM integration improves localization accuracy, enhances mapping responsiveness, and reduces positional uncertainty [7]. Nonetheless, 3D LiDAR-based SLAM remains computationally demanding and requires effective strategies for handling dynamic objects [8]. Beyond localization, 3D LiDAR enhances obstacle detection, terrain mapping, and safe human-robot interaction. Applications span logistics, industrial automation, surveillance, and search and rescue. This research presents the design, development, and implementation of an AMR using 3D LiDAR, advancing toward fully autonomous, intelligent robotic platforms [9].

II. PROBLEM STATEMENT

The emergence of self-driving vehicles and mobile robots demands advanced navigation and localization techniques for real-time dynamic environments. While SLAM technology has progressed significantly, challenges remain in achieving high accuracy, efficiency, and adaptability to real-world conditions. A primary issue is the computational complexity involved in processing sensor data to attain sub-meter precision. This requirement is mathematically expressed by (1):

$$C_{total} = C_{data} \cdot N + C_{a\lg}(D,S) \quad (1)$$

Here, C_{total} denotes the computational cost, C_{data} is the cost of processing a single data point, N denotes the number of data points, $C_{a\lg}(D,S)$ is the algorithmic complexity, dependent on the dataset size D and sensor type S.

Furthermore, the accuracy of localization, crucial for safe navigation, is quantitatively measured by the error metric:

$$E_{loc} = \sqrt{(x_{true} - x_{est})^2 + (y_{true} - y_{est})^2} \quad (2)$$

where (x_{true}, y_{true}) and (x_{est}, y_{est}) represent the true and estimated positions, respectively. Additionally, the adaptability of SLAM systems to dynamic environments introduces the problem of maintaining updated maps, which can be conceptually formulated as:

$$M_{update}(t) = f(M_{t-1}, \Delta E, \Delta O) \quad (3)$$

where $M_{update}(t)$ is the map at time t, M_{t-1} is the map at time $t-1$, ΔE represents environmental changes, and ΔO denotes observed obstacles.

The characteristics of the current methods in the computational, accuracy, and adaptability domains highlight the urgency of innovations that can enhance autonomous driving applications using SLAM systems. This study aims at the development of a framework that reduces the system's computational load, improves navigation accuracy in localized areas, and increases the system's capacity to adapt to environmental changes, thus addressing all the identified problems and advancing navigation technologies in robotics.

III. MATERIALS AND METHODS

The Automated Guided Vehicle (AGV) system was designed to enhance manual environmental mapping by incorporating self-positioning and autonomous navigation using the area's layout map. During assessments, it constructs a map of its surroundings from 3D LiDAR point cloud data, detecting wall features, comparing them with a 2D reference map and wheel odometry, and applying a Monte Carlo particle filter for localization [10]. Sensor integration includes odometry with magnetic encoders for precise displacement via Serial Peripheral Interface (SPI) communication [11] and multidimensional LiDAR for generating detailed point cloud images [12]. This enables accurate localization, obstacle detection, and efficient navigation. The system's architecture comprises three key components: sensor integration, mapping, and navigability optimization (Figure 1).

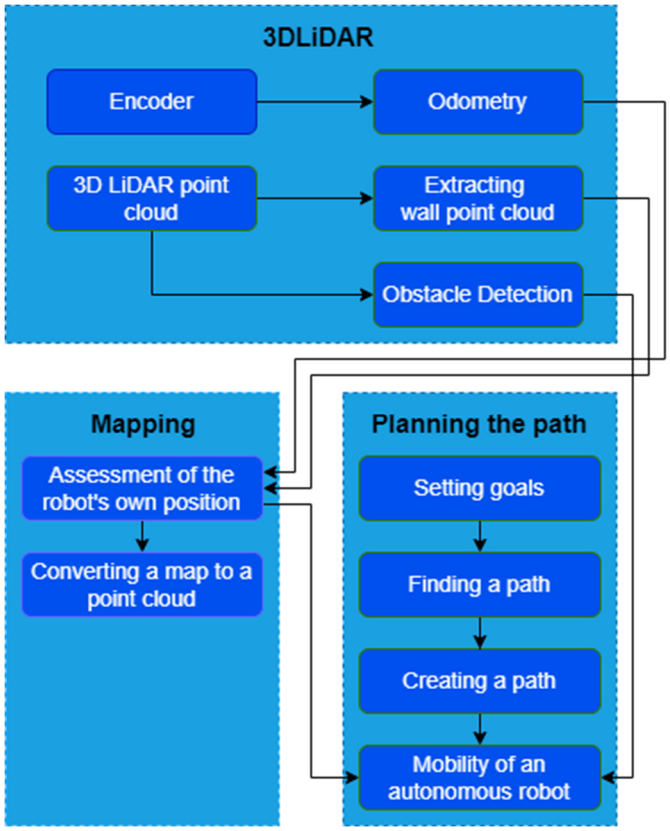

Fig. 1. Basic control scheme of the mobile robot.

In the mapping phase, point cloud data from 3D LiDAR and a layout map are used to refine positioning and incorporate parameters [13]. Identifying walls within the point cloud enhances localization accuracy, whereas Monte Carlo

Localization (MCL) with a particle filter improves alignment between the map model and LiDAR data [14]. During path planning, the system sets a target, applies route-finding methods, and autonomously navigates by detecting goals, selecting optimal routes, and ensuring efficient movement without operational restrictions.

A. The Hardware Module

In this research, the Shenzhen Yahboom Technology Rosmaster X3 Plus mobile robot [15] served as the main experimental platform. Running Ubuntu 20.04 on Robotic Operating System (ROS)-Noetic via VMware, it features a Jetson Orin NX with 16 GB memory for real-time navigation and localization. The YDLIDAR 4ROS LiDAR [16] delivers high-resolution 3D point clouds, complemented by an Astra Pro depth camera, enabling precise perception. This hardware–software integration supports seamless autonomous navigation, making it an effective tool for our study.

Figure 2 demonstrates the AGV system layout, which is based on the two-wheels cart setup. This setup comprises a cart with 3D LiDAR technology and a PC, which is used for data processing. The original setup was modified using a standard bogie, where the front wheels were replaced by the free-wheel casters to make the turnarounds easier, and the rear wheels were upgraded to geared Direct Current (DC) motors to provide the required propulsion.

Fig. 2. Applied mobile robot.

The motor drive mechanism arrangement is shown in Figure 3(a). In addition, a magnetic encoder has been fixed to the platform of the motor, as highlighted in Figure 3(b). The encoder uses a rotating magnet connected to the shaft and a sensor fixed to the housing to measure the shaft's rotation angle without physical contact. The magnetic encoder, providing rotation angle data, is critical for computing the AGV's traveled distance and, consequently, for precise positioning. The key specifications of the hardware components used in the system are summarized in Table I.

TABLE I. COMPONENT SPECIFICATIONS

Component	Specification
DC motor	Voltage: 12 V; Power: 4 W; Rotation speed: 12,000 rpm; Gear ratio: 56:1
Motor driver	Voltage: 3.3–5 V; Current: 4 A; PWM control frequency: 100 kHz; Control voltage: 1.8–5.5 V
Magnetic encoder AS5048A	Voltage: 11 V; Interface: SPI PH2.0 6-pin; Resolution: 14 bit (16,384); Max sampling: 12 kHz
3D LiDAR YDLIDAR 4ROS	Horizontal: 360°; Vertical: 0.13°; Range: 0.05–30 m; Rotation rate: 5–12 Hz; Accuracy: ±3 cm
Jetson Orin NX 16 GB	OS: Ubuntu 20.04; CPU: 8-core Nvidia ARM Cortex; RAM: 16 GB; GPU: 1024 cores Nvidia Ampere; ROS: Melodic

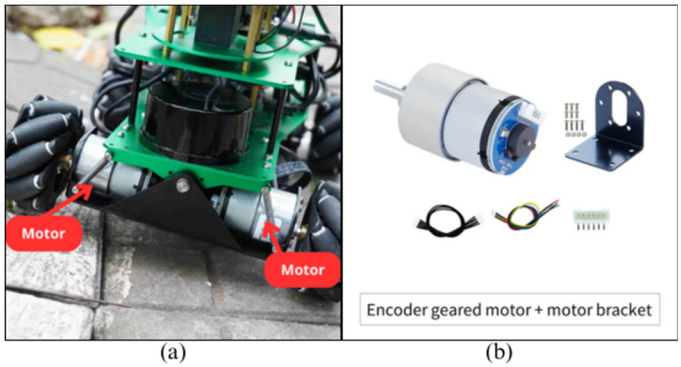

Fig. 3. Motor drive setup: (a) DC motor setup, (b) encoder configuration.

B. Odometry and 3D LiDAR Fusion

The integration of 3D LiDAR and wheel odometry enables the robot to build a detailed understanding of its environment while accurately tracking its movements. Wheel odometry calculates the distance traveled by analyzing wheel rotations, measured through encoders attached to each wheel. Given the wheel radius and the number of encoder ticks, the traveled distance can be mathematically derived. This fusion of odometry with LiDAR data enhances localization accuracy by compensating for drift and ensuring consistent position estimation. If r is the radius of the wheels and N is the number of encoder ticks observed, the distance D traveled by each wheel can be computed as:

$$D = 2\pi r\left(\frac{N}{N_{total}}\right) \quad (4)$$

where N_{total} is the total number of ticks per wheel rotation.

For a two-wheeled robot, the distance traveled D_{avg} and change in orientation $\Delta\theta$ are given by:

$$D_{avg} = \frac{D_L + D_R}{2} \quad (5)$$

$$\Delta\theta = \frac{D_r - D_L}{W} \quad (6)$$

where D_L and D_r are the distances traveled by the left and right wheels, and W is the width between the wheels.

3D LiDAR technology creates a point cloud representing the surroundings. Such data provide a thorough understanding of robot's movement and orientation by giving external reference points. Integrated with the wheel odometry, the LiDAR corrects any drifts and errors that the wheel odometry may accumulate over a period.

The fusion of odometry and 3D LiDAR data utilizes the following approach:

- Initial estimation: Apply wheel odometry to evaluate the robot's movement.
- LiDAR correction: Compare the LiDAR-generated point cloud to the map to identify discrepancies caused by odometry errors.
- Data fusion: Implement a fusion algorithm, for example, the Kalman filter, to integrate odometry and LiDAR data. This process is governed by:

$$\hat{x}_{k|k} = \hat{x}_{k|k-1} + K_k\left(y_k - H\hat{x}_{k|k-1}\right) \quad (7)$$

where $\hat{x}_{k|k}$ is the a posteriori state estimate, $\hat{x}_{k|k-1}$ is the a priori estimate, K_k is the Kalman gain, y_k represents the measurement (LiDAR data), and H is the measurement matrix relating the state to the measurement [17].

- Update position and orientation: Adjust the robot's estimated position (x, y) and orientation (θ) based on the fused data:

$$\begin{aligned} x' &= x + \Delta x \\ y' &= y + \Delta y \\ \theta' &= \theta + \Delta\theta \end{aligned} \quad (8)$$

By integrating wheel odometry with 3D LiDAR data, the robot enhances position and orientation accuracy, minimizing errors from wheel slip or rough terrain. This fusion ensures precise tracking, reliable mapping, and robust autonomous operation, enabling effective navigation in complex, dynamic environments with improved stability and performance.

C. Localization

The 3D LiDAR-enabled navigation of the mobile robot in this study is based on a localization mechanism realized by an accurate algorithm that helps the robot determine its position within its environment. In this section, we explain in detail the mathematical background and internal operation of the localization algorithm utilized in our system, showcasing the integration of 3D scanning data for enchanced node localization accuracy.

- MCL: At the bottom of our localization algorithm lies a common technique known as MCL or particle filter localization. This probabilistic approach utilizes a set of particles to symbolize the robot's possible position and orientation (states) within the environment. Every particle is assigned a weight that reflects the likelihood of the particle's state based on the LiDAR data scan and the robot's motion.
- Particle representation: Each particle i in the set can be represented as:

$$p_i = (x_i, y_i, \theta_i) \quad (9)$$

where x_i, y_i, θ_i denote the particle's position and orientation.

- Weight calculation: The weight w_i is calculated for each particle taking into account the degree of matching between the predicted sensor readings for the particle's state and the actual sensor readings provided by the 3D LiDAR:

$$w_i = P(z_t \mid p_i) \quad (10)$$

where z_t is the LiDAR measurement at time t, and $P(z_t \mid p_i)$ is the likelihood of observing z_t given the state represented by particle i.

- Resampling: Particles are resampled according to their weights, with higher-weight particles being more likely to be selected. This focuses the particle set on the most probable region of the robot's position.
- Incorporation of 3D LiDAR data: Integrating 3D LiDAR data into the MCL algorithm enhances localization accuracy by comparing environmental map details with the map model [18]. The high-resolution point cloud enables precise weight calculation for each particle. The 3D LiDAR sensor model converts sequential point cloud data into a probabilistic format for map comparison, effectively transforming 3D information into 2D data aligned with the map's specifications. This process allows a substantial number of particles to be processed, improving robustness and reliability in localization performance [19].
- Motion update. A motion update is performed before each particle receives a weight calculation according to the robot's reported movement. The particle positions and orientations are updated to reflect the robot's dynamics based on odometry data. The motion model can be expressed as:

$$p_i' = p_i + \Delta p(u_t, \in) \quad (11)$$

where p_i' is the updated particle state, Δp is the change due to the control input u_t at time t, and $\in$ is motion noise.

D. Obstacle Avoidance Algorithm

Obstacle avoidance in autonomous navigation involves two main processes: detecting obstacles and planning an alternative route to bypass them. For instance, if the intended path encounters an obstruction on the left, navigational coordinates are stored as a way-set, each with a defined detection area. This area, modeled as a cylindrical zone around each waypoint, functions as a sensory network for obstacle recognition. Within this range, any detected set point that is not attributed to the ground indicates an obstacle; therefore, the area is non-passable as illustrated in Figure 4.

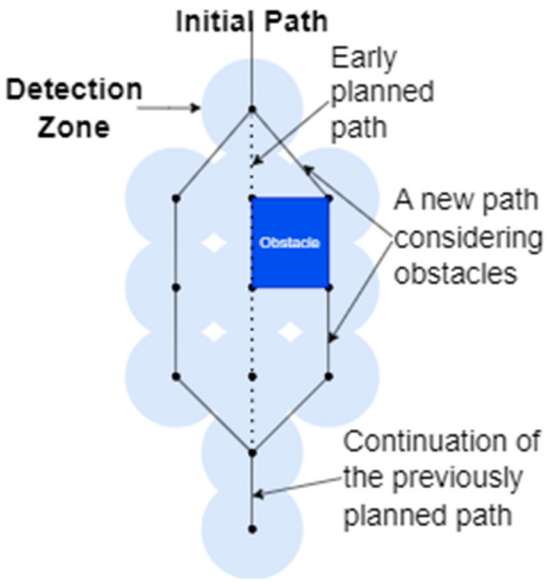

Fig. 4. Obstacle avoidance: The robot detects obstacles within its detection zone and adjusts its path to navigate around the obstacle while continuing along the planned route.

The obstacle avoidance mechanism marks blocked spots and navigates around impediments using mapped alternative corridors. This detection algorithm evaluates possible detours, selecting a contiguous path on one side for the route-finding algorithms to execute. If obstructions block both sides, the vehicle halts until a clear detour is available. This responsive method enables the vehicle to adapt to environmental variability, maneuvering efficiently around obstacles. By integrating real-time detection with dynamic path planning, the system ensures flexible, reliable navigation even in complex and unpredictable operational settings.

IV. EXPERIMENT RESULTS

This section evaluates the accuracy of the generated layout map, which is crucial for reliable self-localization, and assesses the system's overall performance. Validation was conducted against Autoware v1.14.0 [20], an open-source 3D-SLAM platform under the Linux ROS framework [21-23], which uses the Normal Distribution Transform (NDT) matching algorithm [24] for precise scan alignment. Our method was tested by moving a mobile trolley through various factory zones, complemented by ROS-based simulations. This combined real-world and simulated assessment confirms the system's robustness and practical applicability in complex industrial environments.

Figure 5 presents a diagrammatic representation of the navigation process in a two-dimensional environment. Figures 5(a) and 5(b) illustrate the initial stage, where the path-planning phase begins, setting the foundation for subsequent navigation decisions. Figure 5(c) depicts the ongoing path-planning process, highlighting its iterative nature as the robot adjusts its route while moving in different directions. Finally, Figure 5(d) shows the last step, with the finalized map produced at the end of the journey. This sequence of images effectively illustrates the progression from initial path creation to adaptive adjustments during motion, culminating in a complete and accurate map of the traversed path.

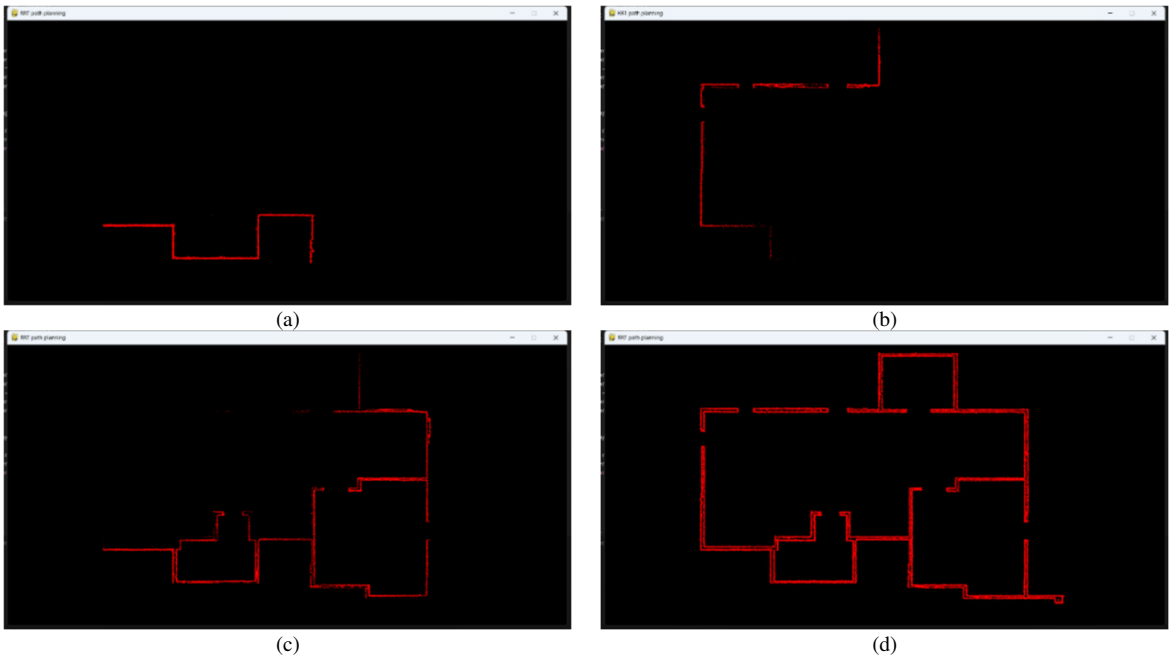

Fig. 5. Path-planning process: (a) planning from left to right, (b) planning from bottom to top, (c) ongoing path-planning process, (d) completed path-planning process.

Figure 6 illustrates the robot's 3D path-planning process, showcasing the steering strategies employed in cluttered environments. The diagram reveals how the system continuously evaluates and adjusts its trajectory in real time, effectively handling diverse terrains and avoiding obstacles. It highlights the robot's ability to perceive and interpret its

surroundings in three dimensions, leveraging advanced algorithms to ensure precise and adaptive navigation. These algorithms enable the generation of a detailed 3D map upon completion of the path. The figure emphasizes the complexity and dynamism of modern 3D path planning, reflecting significant advancements in autonomous vehicle technology toward accuracy and efficiency in challenging environments.

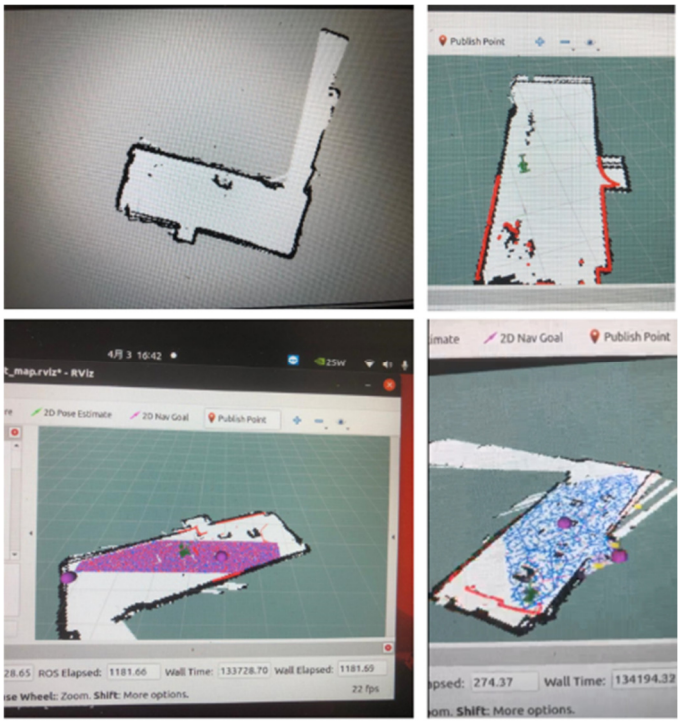

Fig. 6. 3D path planning with multiple viewing angles.

Figure 7 shows the developed mobile robot with an integrated 3D LiDAR sensor operating in a real-world environment, highlighting its design and functional capabilities. The 3D LiDAR provides high-precision environmental perception for real-time navigation, enabling obstacle detection, steering decisions, and accurate localization. As the robot traverses a designated area, it processes LiDAR data to adapt to environmental changes, ensuring safe and efficient movement. This demonstration illustrates the seamless integration of sensing, processing, and control, showcasing the practical application of theoretical designs.

Figure 8 shows the mobile robot performing obstacle avoidance using its 3D LiDAR system. The image captures the moment the robot detects and navigates around obstacles in its path. The 3D LiDAR provides real-time, high-resolution environmental data, allowing precise object detection and enhanced spatial awareness. This enables the robot to dynamically adjust its trajectory for safe navigation. The scenario demonstrates the effectiveness of LiDAR-based obstacle detection and avoidance, highlighting the system's adaptability in complex environments. It exemplifies the integration of advanced sensing and computational technologies, showcasing the developed robot's practical performance and operational efficiency in autonomous navigation tasks.

Fig. 7. Mobile robot navigation using a 3D LiDAR sensor.

Fig. 8. Mobile robot navigation using an integraded 3D LiDAR system.

V. DISCUSSION

This section discusses the results from our study on advanced localization for autonomous navigation, showing improved precision, reliability, and adaptability over existing 3D-SLAM frameworks, especially Autoware's NDT matching, through enhanced sensor fusion and adaptive processing.

A. Comparison with Existing Technologies

The evolution of SLAM technologies has resulted in multiple approaches that differ in sensor input, algorithmic design, adaptability, and operational constraints. Autoware's NDT matching [25] is a well-recognized benchmark for point cloud alignment but struggles in GPS-denied or highly dynamic environments. LiDAR-based SLAM methods [26] improve precision in structured areas but can be computationally expensive.

Adaptive SLAM frameworks [27] address environmental variability, though they may require frequent recalibration. Multi-sensor fusion techniques [28] enhance robustness through diverse data integration but increase system complexity. Cooperative multi-robot SLAM [17] expands coverage but introduces synchronization overhead. OpenStreetMap-based LiDAR localization [29] supports urban scenarios with prior map availability but is less effective in uncharted areas. RadarSLAM [30] delivers high performance in adverse weather conditions but with reduced resolution. Cooperative LiDAR SLAM [24] benefits multi-vehicle networks but depends heavily on communication reliability.

Our proposed method integrates 3D LiDAR with odometry in an adaptive sensor fusion architecture, dynamically weighting sensor confidence and incorporating motion feedback for drift reduction. Empirical and simulated evaluations confirm its superior accuracy, adaptability, and energy efficiency across structured and unstructured indoor–outdoor environments. As summarized in Table II, the proposed method consistently outperforms existing approaches in terms of adaptability, drift compensation, and operational efficiency, particularly in heterogeneous indoor–outdoor environments.

TABLE II. COMPARATIVE ANALYSIS OF LOCALIZATION APPROACHES

Reference & approach	Primary sensor input	Algorithmic approach	GPS-denied environment	Adaptability to dynamic scenes	Energy efficiency	Drift compensation	Tested environments
Proposed method	3D LiDAR + odometry	Adaptive fusion with dynamic weighting + motion feedback	High	High	High	Advanced (feedback loop)	Structured + unstructured (indoor–outdoor)
[25] NDT matching	3D LiDAR	Static point cloud alignment	Moderate	Limited	Moderate	Basic	Structured
[26] LiDAR-based SLAM	3D LiDAR	Iterative scan matching	High	Moderate	Low	Basic	Structured + urban
[27] AdaptSLAM	3D LiDAR	Adaptive mapping algorithms	High	High	Moderate	Moderate	Structured + dynamic
[28] Multi-sensor fusion	LiDAR + IMU + camera	Sensor fusion algorithms	High	High	Low	Moderate	Structured + mixed
[17] Multi-robot cooperation	LiDAR + multi-robot data	Distributed SLAM fusion	High	Moderate	Low	Moderate	Outdoor structured
[29] LiDAR-OSM localization	3D LiDAR + OSM data	Map-assisted matching	High	Moderate	Low	Basic	Structured + urban
[30] RadarSLAM	Radar + LiDAR	Radar-based SLAM	High	High	Moderate	Moderate	All-weather
[24] Cooperative LiDAR SLAM	Multi-vehicle LiDAR	Cooperative SLAM fusion	High	Moderate	Low	Moderate	Outdoor structured

B. Technical Challenges and Solutions

Autonomous navigation in dynamic, cluttered environments faces challenges such as sensor noise, signal loss, and environmental variability. GPS is unreliable indoors, LiDAR struggles with reflective surfaces, and cameras are sensitive to lighting changes [29]. Our approach uses advanced sensor fusion, where each modality compensates for the others' weaknesses. An adaptive fusion algorithm adjusts based on sensor confidence and environmental feedback, ensuring robust localization. Machine learning models improve anomaly detection and correction capabilities. Real-world and simulated tests validated consistent performance across indoor, outdoor, and transitional environments, confirming system reliability [27].

VI. CONCLUSION

This study advances autonomous navigation by introducing an innovative localization system that integrates advanced sensor fusion, adaptive algorithms, and machine learning models to achieve exceptional localization accuracy, efficiency, and adaptability across diverse environments. Comparative evaluations of 2D Simultaneous Localization and Mapping (2D-SLAM) and Normal Distribution Transform (NDT) matching against Autoware demonstrated substantial gains in precision and consistency, particularly in dynamic and unstructured conditions. Comprehensive validation, combining empirical data collection and Robot Operating System (ROS)-based simulations, confirmed the system's robustness and suitability for future unmanned platforms. By addressing core challenges in localization accuracy and system performance, this research supports safer and more reliable autonomous mobility solutions. The proposed system offers broad applicability in domains such as autonomous vehicles, industrial robotics, and aerial drones, with flexibility for urban navigation, industrial automation, and other complex scenarios. Looking forward, the approach establishes a strong foundation for further refinement and integration into next-generation autonomy frameworks. As automation and the Internet of Things (IoT) expand, adopting such technologies will be key to realizing fully integrated, intelligent, and efficient autonomous systems.

ACKNOWLEDGMENT

This work was supported by the Science Committee of the Ministry of Higher Education and Science of the Republic of Kazakhstan within the grant "BR20280990 – Design, development fluid and gas mechanics, new deformable bodies, reliability, energy efficiency of machines', mechanisms', robotics' fundamental problems solving methods."

REFERENCES

[1] R. Dong, Q. Chang, and S. Ikuno, "A deep learning framework for realistic robot motion generation," *Neural Computing and Applications*, vol. 35, no. 32, pp. 23343–23356, Nov. 2023, https://doi.org/10.1007/s00521-021-06192-3.

[2] M. A. A. Noman *et al.*, "A computer vision-based lane detection technique using gradient threshold and hue-lightness-saturation value for an autonomous vehicle," *International Journal of Electrical and Computer Engineering*, vol. 13, no. 1, pp. 347–357, Feb. 2023, https://doi.org/10.11591/ijece.v13i1.pp347-357.

[3] A. Peters and A. C. Knoll, "Robot self-calibration using actuated 3D sensors," *Journal of Field Robotics*, vol. 41, no. 2, pp. 327–346, Mar. 2024, https://doi.org/10.1002/rob.22259.

[4] T. Zhou, C. Zhao, C. P. Wingren, S. Fei, and A. Habib, "Forest feature LiDAR SLAM (F2-LSLAM) for backpack systems," *ISPRS Journal of Photogrammetry and Remote Sensing*, vol. 212, pp. 96–121, Jun. 2024, https://doi.org/10.1016/j.isprsjprs.2024.04.025.

[5] M. Natarajan *et al.*, "Human-Robot Teaming: Grand Challenges," *Current Robotics Reports*, vol. 4, no. 3, pp. 81–100, Sep. 2023, https://doi.org/10.1007/s43154-023-00103-1.

[6] N. Vemuri and N. Thaneeru, "Enhancing Human-Robot Collaboration in Industry 4.0 with AI-driven HRI," *Power System Technology*, vol. 47, no. 4, pp. 341–358, Dec. 2023, https://doi.org/10.52783/pst.196.

[7] V.-H. Le, H.-S. Do, V.-N. Phan, and T.-H. Te, "TQU-SLAM Benchmark Feature-based Dataset for Building Monocular VO," *Engineering, Technology & Applied Science Research*, vol. 14, no. 4, pp. 15330–15337, Aug. 2024, https://doi.org/10.48084/etasr.7611.

[8] S. Mokssit, D. B. Licea, B. Guermah, and M. Ghogho, "Deep Learning Techniques for Visual SLAM: A Survey," *IEEE Access*, vol. 11, pp. 20026–20050, 2023, https://doi.org/10.1109/ACCESS.2023.3249661.

[9] B. J. Zhang and N. T. Fitter, "Nonverbal Sound in Human-Robot Interaction: A Systematic Review," *J. Hum.-Robot Interact.*, vol. 12, no. 4, Dec. 2023, Art. no. 46, https://doi.org/10.1145/3583743.

[10] S.-H. Kang and J.-H. Han, "Video Captioning Based on Both Egocentric and Exocentric Views of Robot Vision for Human-Robot Interaction," *International Journal of Social Robotics*, vol. 15, no. 4, pp. 631–641, Apr. 2023, https://doi.org/10.1007/s12369-021-00842-1.

[11] B. Kulambayev, B. Gleb, N. Katayev, I. Menglibay, and Z. Momynkulov, "Real-Time Road Damage Detection System on Deep Learning Based Image Analysis," *International Journal of Advanced Computer Science and Applications*, vol. 15, no. 9, pp. 1051–1061, Sep. 2024, https://doi.org/10.14569/IJACSA.2024.01509107.

[12] K. Darvish *et al.*, "Teleoperation of Humanoid Robots: A Survey," *IEEE Transactions on Robotics*, vol. 39, no. 3, pp. 1706–1727, Jun. 2023, https://doi.org/10.1109/TRO.2023.3236952.

[13] S. S. Samsani, H. Mutahira, and M. S. Muhammad, "Memory-based crowd-aware robot navigation using deep reinforcement learning," *Complex & Intelligent Systems*, vol. 9, no. 2, pp. 2147–2158, Apr. 2023, https://doi.org/10.1007/s40747-022-00906-3.

[14] D. D. Valluri, "Exploring cognitive reflection for decision-making in robots: Insights and implications," *International Journal of Science and Research Archive*, vol. 11, no. 2, pp. 518–530, Mar. 2024, https://doi.org/10.30574/ijsra.2024.11.2.0463.

[15] "Rosmaster X3 Plus ROS Robot for Jetson NANO 4GB/Orin NX Super/Orin NANO Super/RPi 5." Yahboom. https://category.yahboom.net/products/rosmaster-x3-plus.

[16] "YDLidar 4ROS Lidar system." Yahboom. https://www.yahboom.net/study/YDLIDAR-4ROS.

[17] S. Shen, M. Saito, Y. Uzawa, and T. Ito, "Optimal Clustering of Point Cloud by 2D-LiDAR Using Kalman Filter," *Journal of Robotics and Mechatronics*, vol. 35, no. 2, pp. 424–434, Apr. 2023, https://doi.org/10.20965/jrm.2023.p0424.

[18] S. Ness, N. J. Shepherd, and T. R. Xuan, "Synergy Between AI and Robotics: A Comprehensive Integration," *Asian Journal of Research in Computer Science*, vol. 16, no. 4, pp. 80–94, Sep. 2023, https://doi.org/10.9734/ajrcos/2023/v16i4372.

[19] H. Kuang, X. Chen, T. Guadagnino, N. Zimmerman, J. Behley, and C. Stachniss, "IR-MCL: Implicit Representation-Based Online Global Localization," *IEEE Robotics and Automation Letters*, vol. 8, no. 3, pp. 1627–1634, Mar. 2023, https://doi.org/10.1109/LRA.2023.3239318.

[20] C. Bédard, I. Lütkebohle, and M. Dagenais, "ros2_tracing: Multipurpose Low-Overhead Framework for Real-Time Tracing of ROS 2," *IEEE Robotics and Automation Letters*, vol. 7, no. 3, pp. 6511–6518, Jul. 2022, https://doi.org/10.1109/LRA.2022.3174346.

[21] Y. Chang *et al.*, "LAMP 2.0: A Robust Multi-Robot SLAM System for Operation in Challenging Large-Scale Underground Environments," *IEEE Robotics and Automation Letters*, vol. 7, no. 4, pp. 9175–9182, Oct. 2022, https://doi.org/10.1109/LRA.2022.3191204.

[22] C. Filippini and A. Merla, "Systematic Review of Affective Computing Techniques for Infant Robot Interaction," *International Journal of Social Robotics*, vol. 15, no. 3, pp. 393–409, Mar. 2023, https://doi.org/10.1007/s12369-023-00985-3.

[23] C. Laschi, T. G. Thuruthel, F. Lida, R. Merzouki, and E. Falotico, "Learning-Based Control Strategies for Soft Robots: Theory, Achievements, and Future Challenges," *IEEE Control Systems Magazine*, vol. 43, no. 3, pp. 100–113, Jun. 2023, https://doi.org/10.1109/MCS.2023.3253421.

[24] S. K. Sahoo and B. B. Choudhury, "Autonomous navigation and obstacle avoidance in smart robotic wheelchairs," *Journal of Decision Analytics and Intelligent Computing*, vol. 4, no. 1, pp. 47–66, Feb. 2024, https://doi.org/10.31181/jdaic10019022024s.

[25] S. O. Ajakwe, D.-S. Kim, and J.-M. Lee, "Drone Transportation System: Systematic Review of Security Dynamics for Smart Mobility," *IEEE Internet of Things Journal*, vol. 10, no. 16, pp. 14462–14482, Aug. 2023, https://doi.org/10.1109/JIOT.2023.3266843.

[26] S. Fang, H. Li, and M. Yang, "LiDAR SLAM Based Multivehicle Cooperative Localization Using Iterated Split CIF," *IEEE Transactions on Intelligent Transportation Systems*, vol. 23, no. 11, pp. 21137–21147, Nov. 2022, https://doi.org/10.1109/TITS.2022.3174479.

[27] Y. Chen, H. Inaltekin, and M. Gorlatova, "AdaptSLAM: Edge-Assisted Adaptive SLAM with Resource Constraints via Uncertainty Minimization," in *IEEE INFOCOM 2023 - IEEE Conference on Computer Communications*, New York City, NY, USA, 2023, pp. 1–10, https://doi.org/10.1109/INFOCOM53939.2023.10229009.

[28] Y. Cho, G. Kim, S. Lee, and J.-H. Ryu, "OpenStreetMap-Based LiDAR Global Localization in Urban Environment Without a Prior LiDAR Map," *IEEE Robotics and Automation Letters*, vol. 7, no. 2, pp. 4999–5006, Apr. 2022, https://doi.org/10.1109/LRA.2022.3152476.

[29] M. Elhousni, Z. Zhang, and X. Huang, "LiDAR-OSM-Based Vehicle Localization in GPS-Denied Environments by Using Constrained Particle Filter," *Sensors*, vol. 22, no. 14, Jul. 2022, Art. no. 5206, https://doi.org/10.3390/s22145206.

[30] Z. Hong, Y. Petillot, A. Wallace, and S. Wang, "RadarSLAM: A robust simultaneous localization and mapping system for all weather conditions," *The International Journal of Robotics Research*, vol. 41, no. 5, pp. 519–542, Apr. 2022, https://doi.org/10.1177/02783649221080483.